Pergamon

Computers Math. Applic. Vol. 28, No. 10–12, pp. 175–208, 1994

0898-1221/94 $7.00 + 0.00

0898-1221(94)00192-8

Collisions of Microdrops of Water

B. WYATT*
Bell Helicopter
Fort Worth, TX, U.S.A.

Abstract—In this paper, collisions of microdrops of water were studied. Experimental studies of microdrops become very difficult as the drop dimensions become extremely small, particularly when the drops are so small that they contain only a few thousand molecules. To overcome these physical limitations, we produced a model for the H_2O molecule using molecular and atomic interaction forces. We then placed these molecules together to produce drops. Hence, using this new technique, we could study drops with no lower size limitations.

To study the motions of these drops, large systems of second order nonlinear ordinary differential equations had to be solved numerically. The system of equations were solved using a CRAY Y-MP8/864 computer. To observe the motion of the drops, output data was transferred to a SGI IRIS 4D-70/GT graphics computer which drew three-dimensional pictures of the data.

Keywords—Microdrop, Collision, Coalescence, Nucleation, Lennard-Jones potential, Oscillation, Dissociation.

1. INTRODUCTION

Microdrop collisions are important in understanding rain drop shapes and oscillations, which in turn are important in understanding how rain storms polarize electromagnetic signals such as radio and microwave transmission. For example, if two communication channels transmit at close to the same frequency, but are polarized differently, the polarization of a rain storm can cause "crosstalk" [1].

Microdrop collisions are also important in the actual formation of rain drops themselves. Clouds are formed as rising warm air, saturated with water vapor, cools and the water vapor condenses on water attracting nucleation sites, such as small suspended salt and dust particles, to form cloud droplets. The rate of increase in the size of cloud droplets by condensation slows as the droplets become larger. As a result, condensation tends to produce many small drops rapidly, but is slow in creating large ones. Therefore, if condensation alone were to produce rain drops, hours would be needed to generate a rain drop large enough to fall through the updraft of the cloud and reach the ground before evaporating. Since rain storms can start from a clear sky in less than an hour, some process other than condensation must be producing the larger drops. One such process is collision and coalescence of cloud droplets. Large drops have a greater mass to surface area ratio than small drops, which gives larger drops a smaller air resistance to mass ratio. Consequently, they have a faster terminal velocity. As a result, they overtake, collide, and coalesce with smaller drops, increasing their mass and velocity as they fall [2–6].

Even more fundamental than the creation of rain drops are the interactions of the extremely minute drops produced by nucleation, as in cloud formation. Experimental studies at these dimensions are very difficult, particularly when the drops contain only a few thousand molecules [7]. But recently, with the availability of fast computing systems, studies of water using computer

*Address for correspondence: 5612 Bransford Rd., Colleyville, TX 76034, U.S.A.

simulated molecular interactions have enabled scientists to study phenomena down at this level, which has, thus far, eluded experimental measurements [8,9].

Many physical experimental studies [10–12] of small water drop collisions have been done. Scientists have studied such things as the effects of size, velocity, impact variables, and other parameters on whether colliding drops will bounce apart, coalesce permanently, coalesce then separate, spatter, or have some other outcome. But because of physical limitations, drops of a radius of less than 60 micrometers were not able to be generated with any consistency. From the molecular point of view, a drop with a radius of 60 micrometers is still quite large, containing roughly 3×10^8 molecules. The largest cloud droplets seldom have a radius of more than 20 micrometers [13] and the average cloud droplet can be a giant compared to the initial drops formed by nucleation. Therefore, the actions of very small drops have not been studied in a physical way.

In our study, a supercomputer was used to model water drops using molecular interaction forces. Hence, the size of a drop is limited from above only by a number of molecular interactions the computer can simulate in a reasonable time period, and is limited from below only by the size of a single molecule. Studies have shown that computer simulations of water yield many of the key attributes of water. These computer simulations of water, as well as of other liquids, are being used extensively to find answers to questions in many fields that are not accessible by physical experiments [9].

2. DEVELOPMENT OF A MODEL FOR THE WATER MOLECULE

The first task we had was to choose or create a model for the water molecule from which our drops would be constructed. There are basically four types of water molecule models being used today:

1. Single point models, such as the Gaussian core model (GCM) [14,15] and those that use a lone Lennard-Jones potential type site [16];
2. Multiple point rigid models, such as the ST2 [17], the TIP series [18–20], and the SPC [18,21,22];
3. Flexible models such as the central force model (CFM) [8,23,24]; and
4. Polarizable models [25,26].

The single point models are the least computer-intensive, but lack structure. The GCM, for example, is only a repulsive model and must be held together by boundary constraints. The lone Lennard-Jones type models do allow for attraction and repulsion between molecules, but by having only a single interaction site, they cannot model the polar structure of water.

The multiple point rigid models, because they have more than one interaction site, are able to model the polar structure of water. It is this polar structure that gives water its many unique and interesting properties. These models are the most widely studied and are less computer-intensive than the flexible or polarizable models, but they do not allow for intramolecular vibrations.

The flexible models produce polar molecules, and also allow for intramolecular vibrations and molecular dissociation. To pay for all of these freedoms, the flexible models tend to consist of very complex functions which do not vectorize well.

All of the multiple point rigid models and the flexible models cited above use effective pair potentials which take into account that interaction potentials are not pairwise additive. In other words, interaction potentials are not simply the summation of all the isolated pair potentials, but are a result of many-body effects. To incorporate these many-body effects, the effective pair potentials use the average nonadditive character of the interactions. This gives a pairwise additive model of the water molecule, whose single molecule structure is slightly different than that of true water, but whose bulk structure is correct. The alternative to using an effective pair potential is to create a non-pairadditive model, which is what the polarization models are attempting to do. These models take into account that the oxygen and hydrogen atoms do not

possess spherically symmetric charges. The oxygen atom, in particular, possesses a nonnegligible electron cloud whose orientation is a consequence of the positions of all the atoms in the system. As a result of this electron cloud shifting, each oxygen atom will be polarized and have an ever changing dipole moment [25]. However, these models are relatively recent, very complex, and are not as well developed as the other models [27].

Because we were studying the collisions of microdrops of water, we wanted the molecules to be able to have internal vibrations to absorb some of the kinetic energy of the collisions. Therefore, a flexible model such as the CFM seemed to be a good choice. On the other hand, to create a drop of a reasonable size, a large number of molecules are needed and this can very quickly yield an overwhelming computational task. This indicated that a less computer intensive rigid model, such as the SPC, would be desirable.

The only liability of the SPC was that it is not flexible. The major liability of the CFM was that its functions are very complicated and do not vectorize well. One of the main reasons that the functions of the CFM are so complicated is that the model allows the molecule to dissociate into ionic components. Since dissociation rarely happens under ordinary circumstances (about one in 10^7 molecules [8], it was of very little importance in our studies.

To obtain all of the properties, we desire without the liabilities noted, we produced a new hybrid model (HYB) which took features from both the CFM and the SPC. This model allows intermolecular vibration, but does not spend time on molecular dissociation and ionic components, which makes it more cost effective.

To create the HYB model, we used the exact specifications of the SPC because of their simplicity. But, instead of placing them on a rigid molecule, we placed them on a dynamic molecule, that itself is held together by Lennard-Jones potential sites, which can be easily vectorized. When the molecule is vibrating, on average, it is effectively the SPC model, and when the atom is in its minimum energy state, it has exactly the same dimensions as the rigid SPC model. See Figure 1.

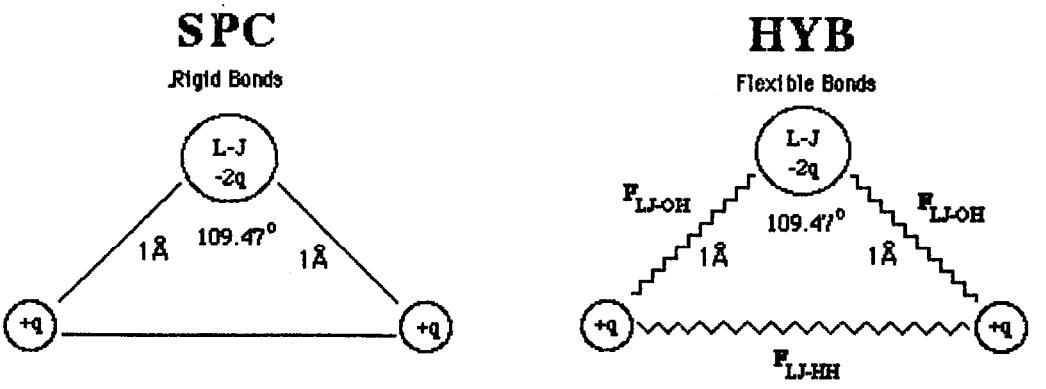

Figure 1.

In this study, to keep numbers used in calculations as close to unity as possible, units were defined as follows: distance in angstroms Å, mass in atomic mass units u, and time in picoseconds ps. This resulted in more rapid computer calculations and an increased accuracy.

The SPC has point charges of $+q$ placed at the centers of the hydrogen atoms and a point charge of $-2q$ located at the center of the oxygen atom. The charge q is equal to 0.41e. A Lennard-Jones interaction site that acts between oxygen atoms is also located at the center of the oxygen atom. The hydrogen atoms are both one angstrom away from the oxygen atom and the HOH angle is 109.47 degrees.

The Coulombic force between atoms of different molecules is given by:

$$F_c(r) = \frac{q_1 q_2}{r_2},$$

where q_1 is the charge on the first atom and q_2 is the charge on the second atom.

The Lennard-Jones interaction site has a minimum potential P_0 when the oxygen-oxygen separation distance is r_0. The Lennard-Jones potential has the following form:

$$P_{LJ}(r) = -P_0 \left[\left(\frac{r_0}{r}\right)^{12} - 2\left(\frac{r_0}{r}\right)^{6} \right],$$

where $P_0 = -65.02$ uÅ/ps^2, and $r_0 = 3.5532186$ Å.

Since the force generated by a potential field is given by the negative derivative of the potential, the accompanying force function of the Lennard-Jones site is the following:

$$F_{LJ}(r) = \frac{-12P_0}{r_0} \left[\left(\frac{r_0}{r}\right)^{13} - \left(\frac{r_0}{r}\right)^{7} \right].$$

A graph of this force function is given in Figure 2.

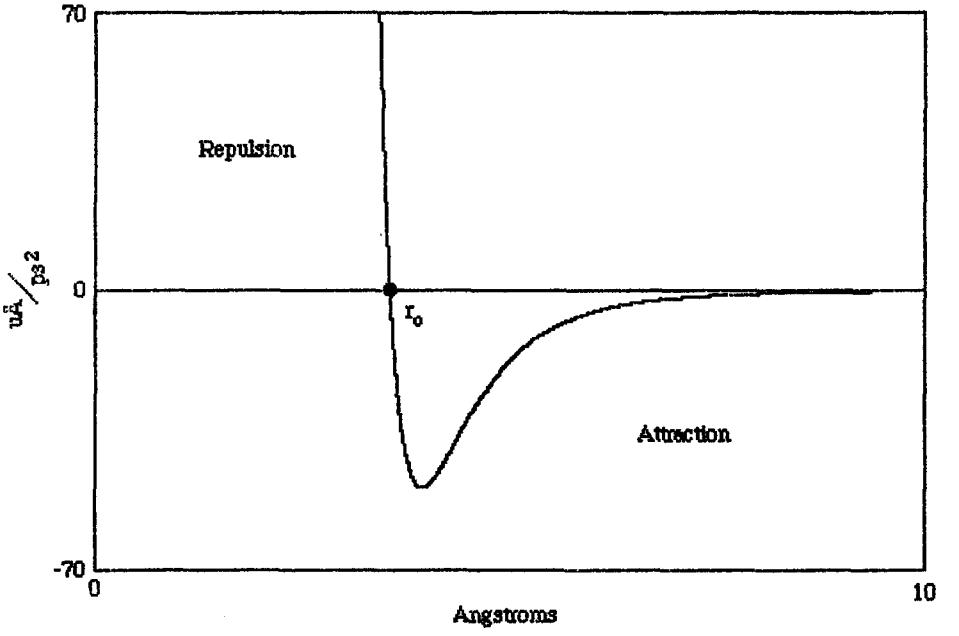

Figure 2.

The SPC specifications provided for the molecule-molecule interactions. Next, we needed to take care of the internal atom-atom interactions that hold the molecule itself together. This needed to be done in such a way that when the molecule is in its minimum energy state, it would have the same configuration as the rigid SPC molecule. To do this, we needed to simulate the covalent OH bounds with minimum potentials occurring when the oxygen-hydrogen separation is one angstrom, and employ a force to keep the two hydrogen atoms 1.6329808 Å apart, on average, to produce the desired HOH angle of 109.47 degrees.

To form the OH bonds, we placed Lennard-Jones potential sites on the oxygen and hydrogen centers with r_0 equal to one angstrom. The hydrogen atoms were kept apart at the proper distance by placing Lennard-Jones potential sites at the hydrogen centers with r_0 equal to 1.6329808 Å. It is very important to note that these additional potentials only act between atoms in the same molecule. For the minimum values of these potentials, we used the experimental values of the covalent OH bond and the covalent HH bond [28]. Hence,

$$P_0 = -42760.48\,\text{uÅ}^2/\text{ps}^2, \text{ for the OH bond}$$

and

$$P_0 = -43608.96\,\text{uÅ}^2/\text{ps}^2, \text{ for the HH bond.}$$

The mass of the oxygen atom was taken to be 16u and the mass of each hydrogen atom was taken to be 1u.

3. MATHEMATICAL FORMULATION

If a drop of M molecules was to be created using the preceding force functions to govern molecular and atomic interaction, then to observe the drop's motion, the locations of a total of $3M$ atoms had to be determined through time. Since effective pair potentials were used, and from the fact that point charges and Lennard-Jones sites were located at mass centers, forces on any atom in the drop, at any fixed time, could be completely determined by the position of its center of mass relative to every other atom's center of mass. Therefore, the total force on any given atom, at any given time, could be found by summing up all of the $3M - 1$ isolated forces on that atom caused by every other atom in the drop. Hence, for given initial positions and velocities, the motion of each atom, which in turn generated the motion of the drop, was given by the coupled system of second-order ordinary differential equations:

$$\frac{d^2\mathbf{r}_i}{dt^2} = \frac{\mathbf{F}_i}{m_i}, \qquad i = 1, 2, \ldots, 3M,$$

where $\mathbf{F}_i$ was the force vector, m_i was the mass, and $\mathbf{r}_i$ was the position vector of the i^{th} atom. This was a Newtonian $3M$ body problem, which in general could not be solved analytically for given initial data, so that it had to be solved numerically [29,30].

In choosing a numerical model to solve this system, large time steps needed to be avoided since the force functions created by the Lennard-Jones potentials used high powers of r_0/r_{ij}, where r_{ij} is the distance between the i^{th} and j^{th} atoms, and r_{ij} could be very small. Hence, large time steps could have caused exponential overflows or unnaturally explosive molecules and drops. Therefore, the use of high-order numerical methods, which allow the use of large time steps, would have been counter productive. So we used the simple, but stable, leap-frog formulas to solve this system of equations [29]. Other methods of solving the system are discussed in [30].

To describe the process, let Δt be the positive time step, $t_k = k\Delta t$, $k = 1, 2, \ldots$, and N be the number of atoms. Now, let m_i be the mass of the i^{th} atom and let $\mathbf{F}_{i,k}$, $\mathbf{a}_{i,k}$, $\mathbf{v}_{i,k}$, and $\mathbf{r}_{i,k}$ be the force, acceleration, velocity, and position vectors of the i^{th} atom, respectively, at time t_k for $i = 1, 2, \ldots, N$. Then the leap-frog formulas are:

$$\begin{aligned}
\mathbf{v}_{i,1/2} &= \mathbf{v}_{i,0} + \frac{\Delta t}{2}\mathbf{a}_{i,0}, && \text{(starter formula)} \\
\mathbf{v}_{i,k+1/2} &= \mathbf{v}_{i,k-1/2} + (\Delta t)\,\mathbf{a}_{i,k}, && k = 1, 2, 3, \ldots \\
\mathbf{r}_{i,k+1} &= \mathbf{r}_{i,k} + (\Delta t)\mathbf{v}_{i,k+1/2}, && k = 1, 2, 3, \ldots \\
\text{where } \mathbf{a}_{i,k} &= \frac{\mathbf{F}_{i,k}}{m_i}, && k = 1, 2, 3, \ldots, \text{ and } i = 1, 2, \ldots, N.
\end{aligned}$$

The time step, Δt, for this study was set at .0002 ps.

Because of the importance of the hydrogen bond to the properties of water, a dimer, trimer and tetramer produced by the HYB model are shown in Figure 3. The dimer shows the most stable configurations of two water molecules. In this configuration, one molecule is a hydrogen donor and the other is a hydrogen acceptor. The remaining three hydrogen atoms which are not part of the bond arrange themselves in such a way that their separation is maximal, subject to the constraint of preserving the HOH angles. The trimer is an example of a closed chain that contains a double donor molecule, and a donor-acceptor molecule. The tetramer is an example of a closed cyclic donor-acceptor molecule chain.

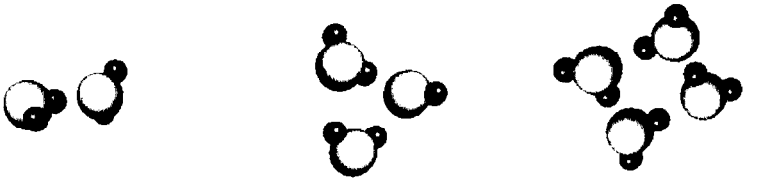

Figure 3.

4. BUILDING THE DROPS

For our experiments, we needed two stable drops of water near room temperature (300 K), which we would call drops A and B. Economic constraints limited us to drops of around 700 molecules. To build drop A, we placed the centers of mass of the water molecules three angstroms apart on the nods of a square lattice, 24 angstroms to a side, for a total of 729 molecules. The HOH planes of the molecules were all parallel and the hydrogen atoms hung down one angstrom from their parent oxygen atoms at 55 degrees off vertical on each side. (See Figure 4.)

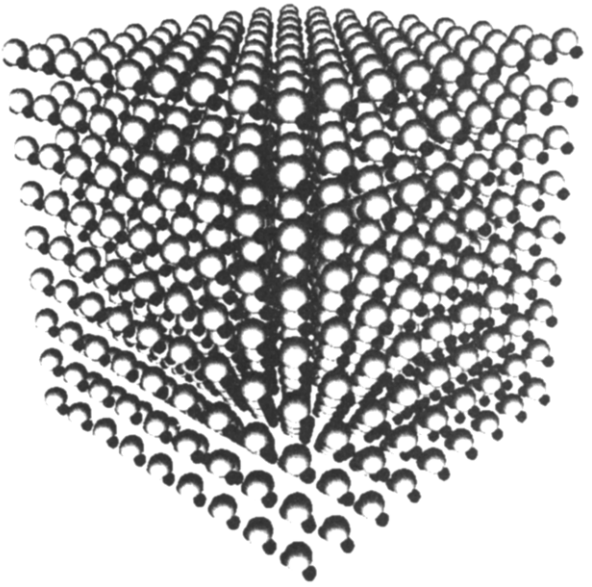

Figure 4.

The molecules in this unnatural configuration had a great deal of potential energy. To remove this excess energy, this unstable drop was allowed to run for many time steps with the application of an additional damping force that severely retarded velocity. This force kept the drop from exploding and allowed the molecules to work their way into more natural positions that possessed much less energy. The molecules were also given some angular and linear velocities to agitate the system so that they would not get caught in unfavorable positions.

The stable drop that we obtained from the above procedure now had to be brought to approximately 300 degrees Kelvin. The equipartition theorem was used to define the temperature in degrees Kelvin as $2/(3k)$ times the total kinetic energy divided by the total number of atoms in the system, where k is the Boltzmann constant [31]. Since the temperature is a function of kinetic energy, to bring the drop to 300 K, kinetic energy had to be added or taken away from the system. This was accomplished by adding the following velocity adjusting force function to each atom of the system:

$$F(v, T_n) = -c(T_n - 300)\, v,$$

where c was a positive constant that determined how severe the force would be; T_n was the average temperature of the system taken over n time steps; and v was the velocity of the atom. Several runs were made each time, decreasing c and increasing n, to fine tune the system to 300 K. After each run, the average velocity had to be reset to zero because the added function caused the average velocity to drift away from zero, which affected the true temperature of the drop. The center of mass of the drop also drifted. This drift did not affect the temperature, but the center of mass was also reset to zero to keep track of its location.

After our drop was adjusted to 300 K, all external forces were removed and the drop was allowed to run freely for a few picoseconds to remove the after-affects of the temperature adjusting

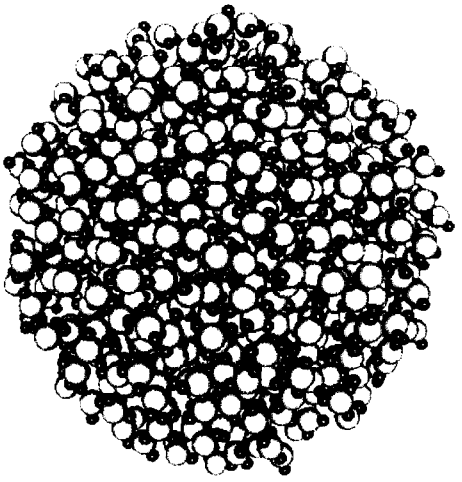

Figure 5.

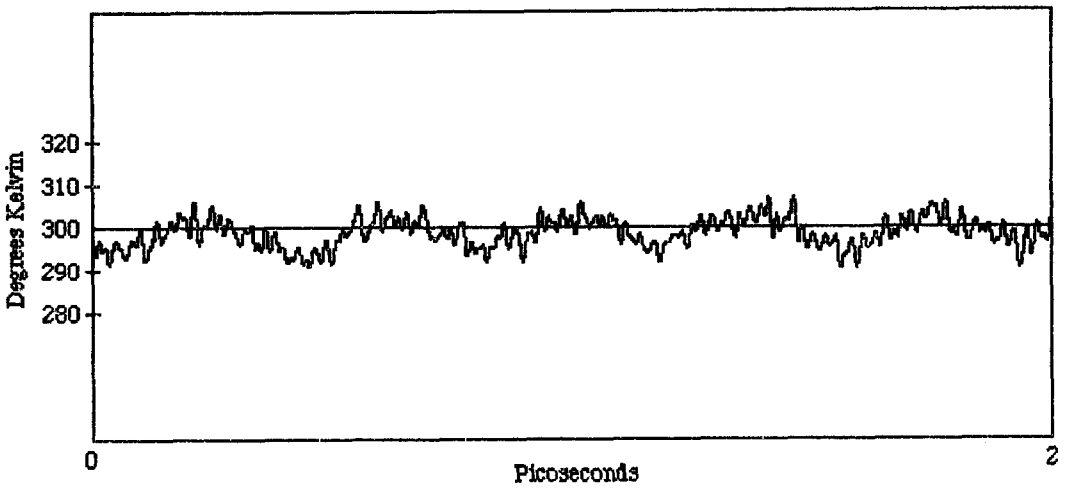

Figure 6.

function. The final positions and velocities of the above drop were then defined as the initial positions and velocities of drop A. Drop A is pictured in Figure 5.

A temperature profile was taken of drop A with readings recorded every time step for 2 picoseconds. A graph of this profile is given in Figure 6. As can be seen from this profile, the temperature of the drop oscillated consistently around 300 K.

To diminish symmetric effects in our collision experiments, drop B should not be identical to drop A. To accomplish this without using any more computer time, we defined the final positions and velocities of drop A, after the temperature profile, to be the initial positions and velocities of drop B. In other words, the two drops were the same except that drop B was two picoseconds older than drop A.

5. COMPUTER EXPERIMENTS

Explanation of experimental setup:

The following computer experiments were run on a CRAY Y-MP8/864 computer. The output was gathered and pictured using a SGI IRIS 4D-70/GT graphics computer. Drop A is pictured with black oxygen atoms and drop B is pictured with white oxygen atoms. For the collisions pictured in Computer Experiments 1–5 and 7, the right side of the page is the positive x direction, the top is the positive y direction, and the normal toward the reader is the positive z direction. For the collision pictured in Computer Experiment 6, the setup was rotated 90 degrees clockwise

about the z axis. The separation between drops was defined as the minimum distance between the geometric centers of atoms from different drops. In each computer experiment, the y and z components of the centers of mass of each drop were the same, and the x components of the centers of mass of each drop were adjusted so that the drops would be the desired distance apart. Drop velocity was defined as the average velocity of each atom in the drop, i.e., the bulk velocity of the drop. All times listed in the experiment are in picoseconds.

Experiment 1

In the first run, we placed drops A and B three angstroms apart with zero drop velocities. This showed how drops, with little or now relative velocity to each other, and in very close proximity to one another, will coalesce and form one drop.

The resultant drop oscillated smoothly between vertical and horizontal elongations. The oscillation damped very rapidly as this motion was transformed into an increase in random velocities of the molecules, and the drop became spherical. Experiment 1 is shown in Figures 7–9.

Experiment 2

In this run, drops A and B were placed 44 Å apart with no initial drop velocities. This showed how extremely small suspended droplets, separated by several radii, will attract and coalesce with one another.

This attraction between droplets is caused by molecular forces whose strength decreases rapidly as separation increases. Therefore, it should not play a major role in the coalescence of droplets the size of cloud droplets, unless they are very close together. During the nucleation stage, however, when clouds are being formed, it should be very important. For it is at this stage that many minute drops are being formed, with very small separations, by condensation of water vapor. This experiment shows why drop growth is so rapid during the initial stages, but slows dramatically as the drops get larger.

Experiment 2 is shown in Figures 10–13. The oscillations of this experiment were much the same as Experiment 1, but were more severe since the greater separation allowed more impact velocity to be generated. Note the speed with which these drops coalesced. The entire process took less than 5 picoseconds. To get a feel for how fast this is, let us compare it to the clock cycle of the new CRAY C90 supercomputer which is 4 nanoseconds. Hence, the drops in this experiment could start with zero velocity, attract, collide, coalesce, oscillate, and damp to a spherical drop 1250 time in one clock cycle of the CRAY C90.

Experiment 3

In this run, drops A and B were placed 3 Å apart. Drop A had a velocity vector of (3,32,0) Å/ps and drop B had a velocity vector of (-3,-32,0) Å/ps. These conditions caused an indirect collision that was very close to the limits for which drops of this size can coalesce. Note that these limits are extremely high. Each drop had a velocity of around 7200 miles per hour.

The drops collided, stretched apart, then coalesced into a single dumbbell shaped drop with a very narrow handle, and began to rotate as linear momentum from the two separate drops was transformed into angular momentum of the resultant drop. As the drop rotated, the molecules near the center of rotation had the smallest angular velocities. As a result, the centripetal force was weaker on molecules closer to the center of rotation. Hence, the attractive forces of the molecules in this region overpowered the centripetal force and caused molecules to gather towards the center. As the molecules gathered, the drop's dumbbell shape became more and more ellipsoidal.

This gathering of molecules had a negative effect on drop coalescence, because, as the molecules gathered in the center, the moment of inertia of the system was reduced. This caused the system

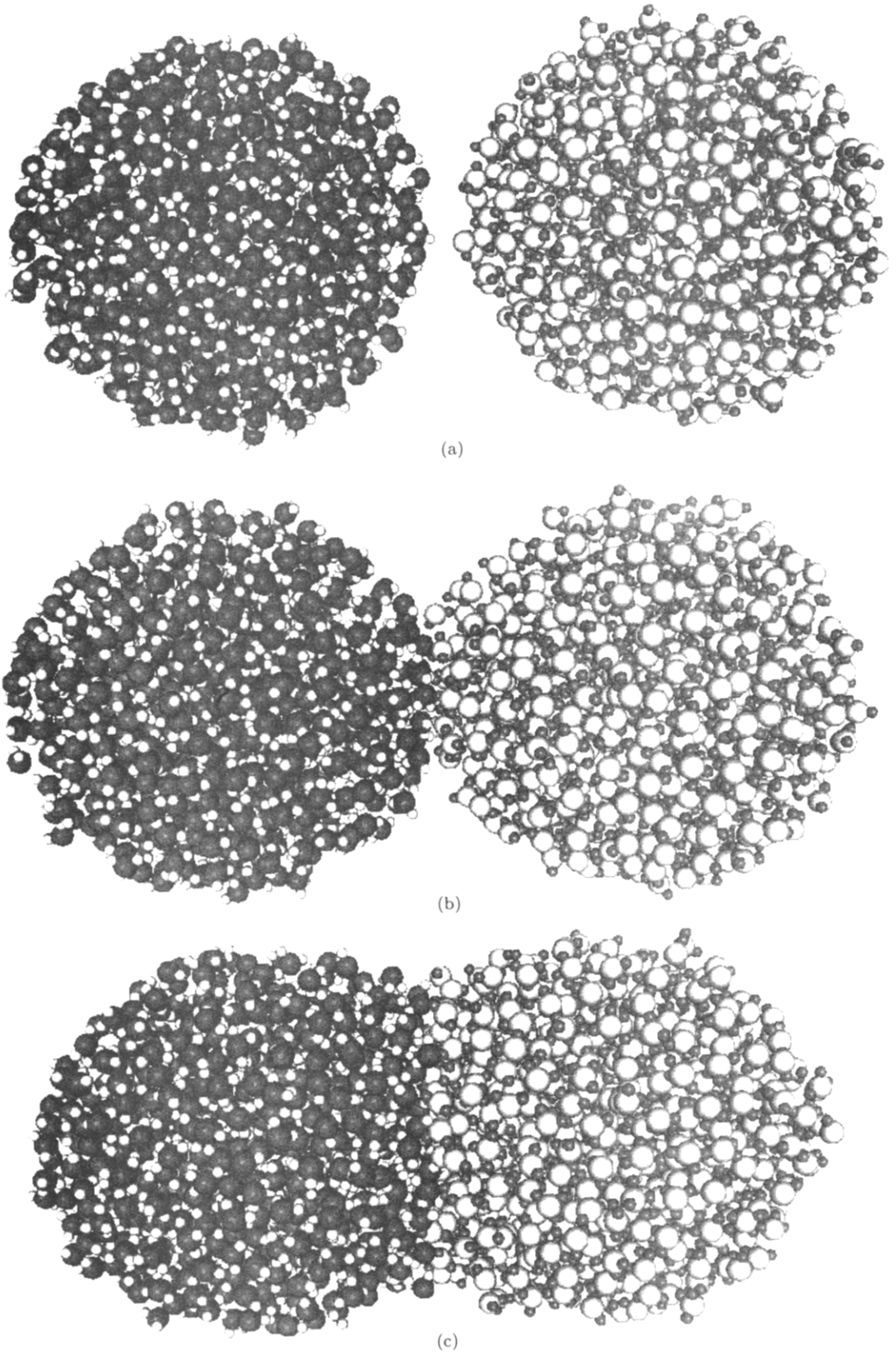

Figure 7. (a) Time = 0.0. (b) Time = 0.2. (c) Time = 0.4.

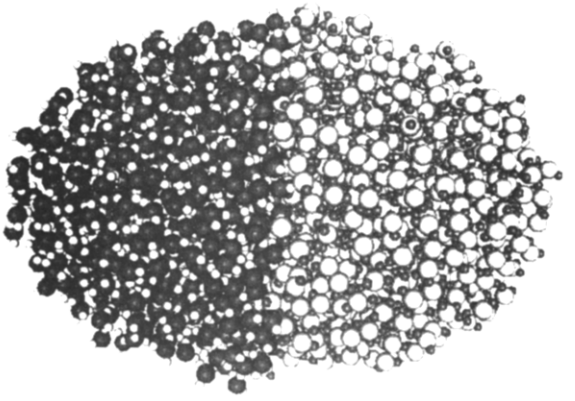

(d)

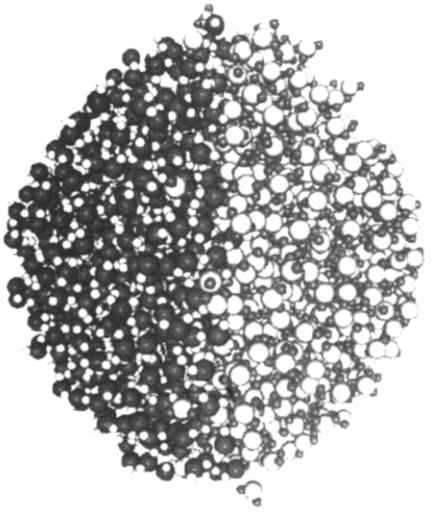

(e)

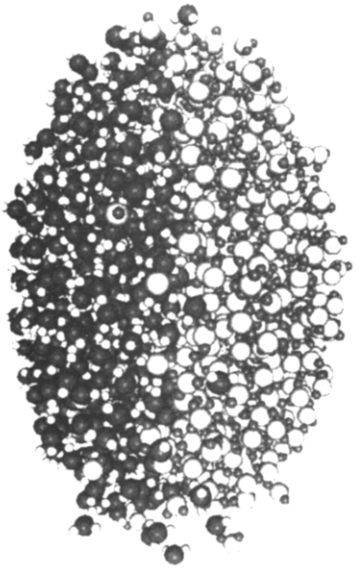

(f)

Figure 8. (d) Time = 0.6. (e) Time = 0.8. (f) Time = 1.0.

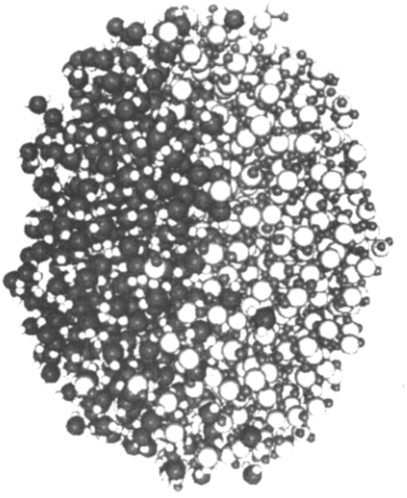

(g)

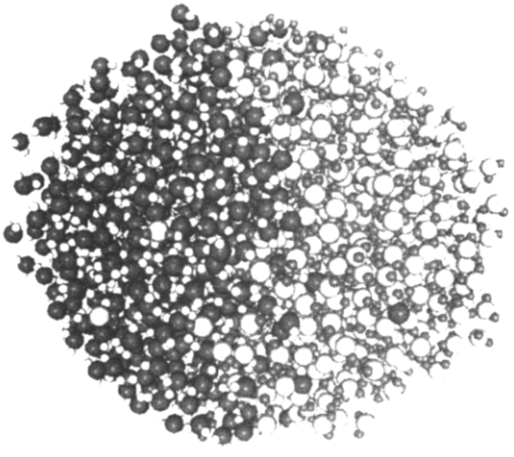

(h)

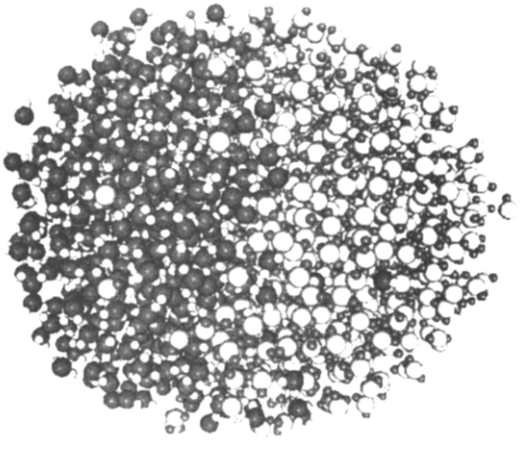

(i)

Figure 9. (g) Time = 1.4. (h) Time = 1.8. (i) Time = 2.2.

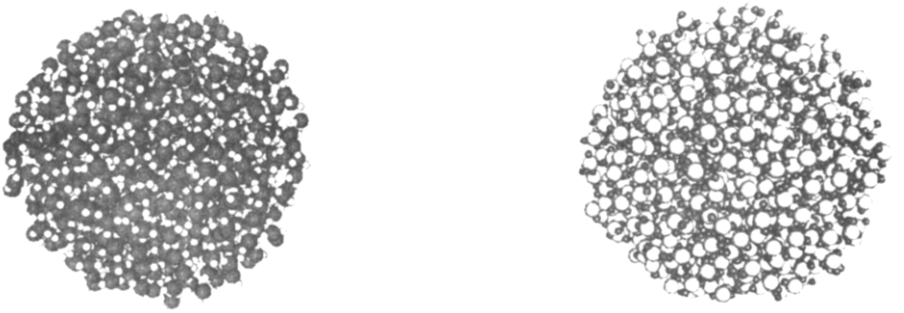

(a)

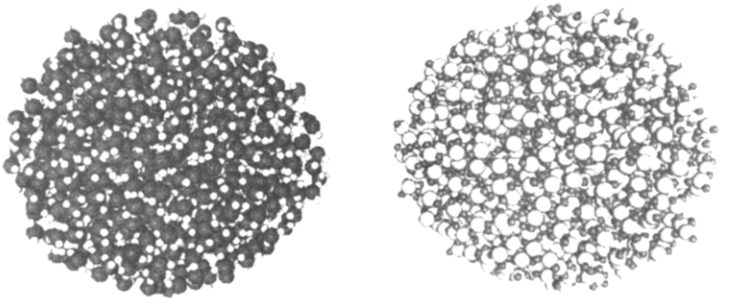

(b)

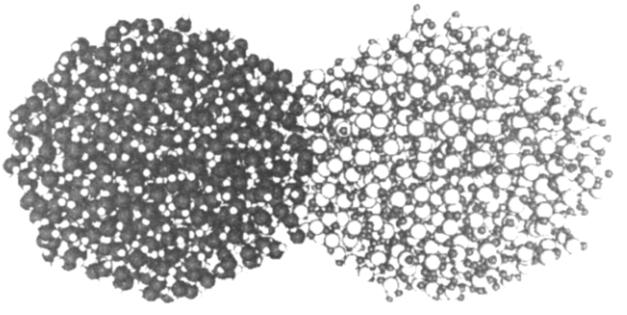

(c)

Figure 10. (a) Time = 0.0. (b) Time = 1.8. (c) Time = 2.0.

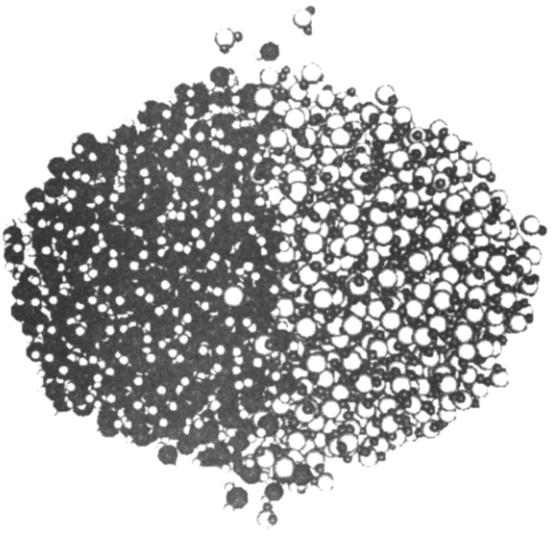

(d)

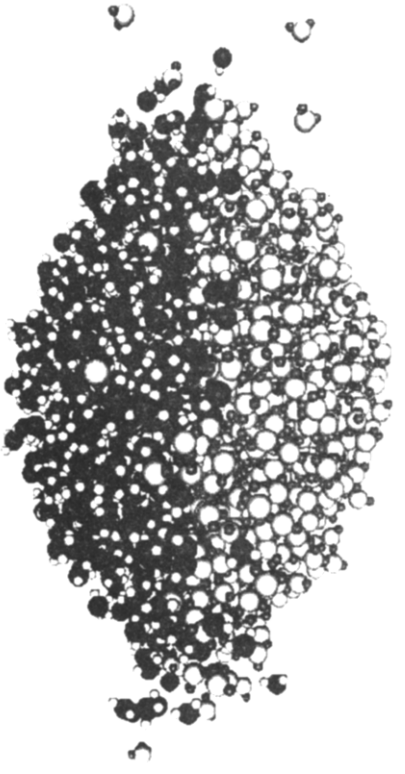

(e)

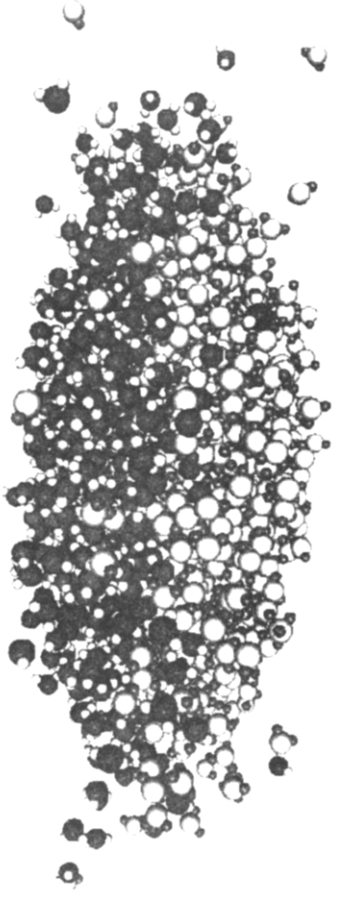

(f)

Figure 11. (d) Time = 2.2. (e) Time = 2.4. (f) Time = 2.6.

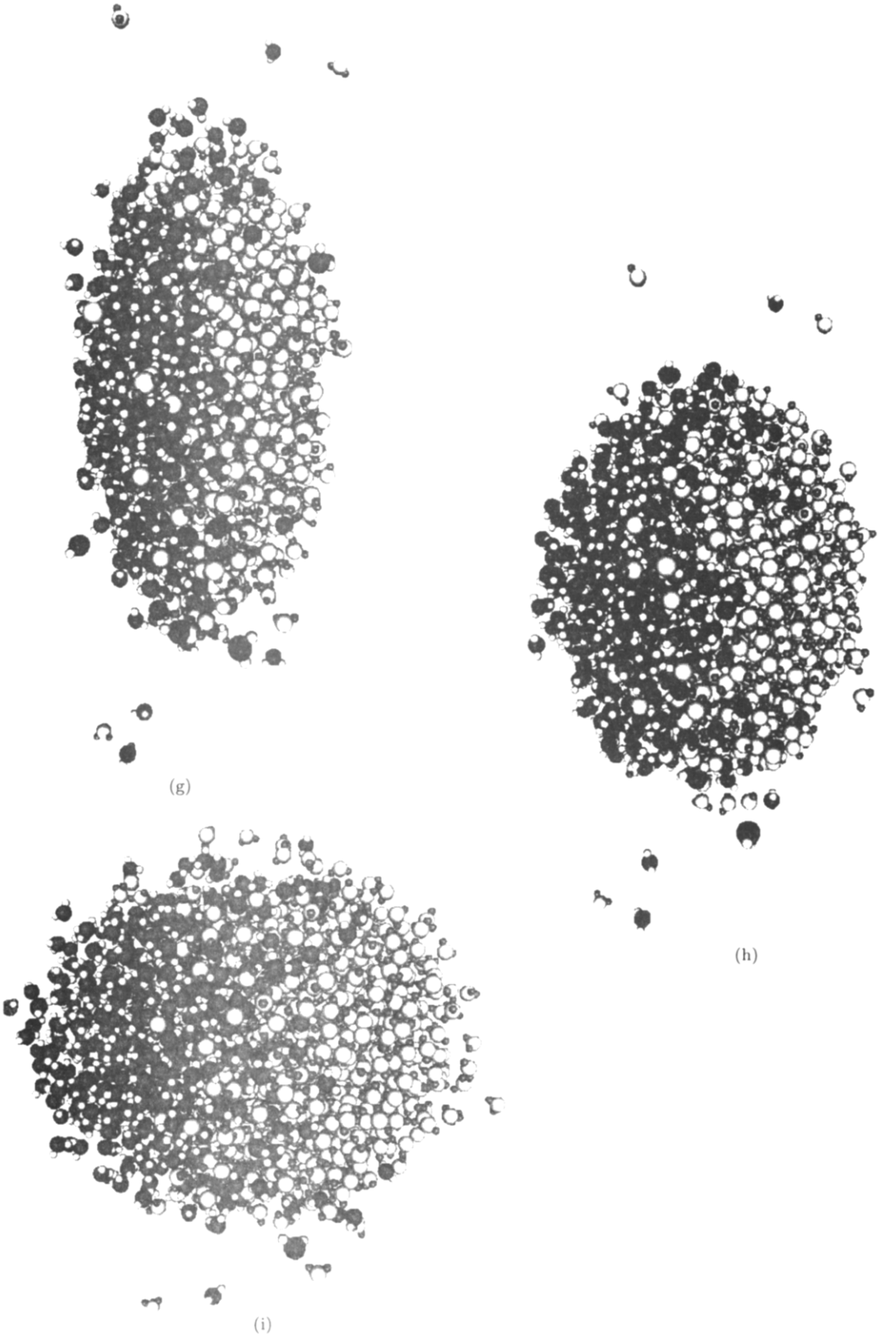

Figure 12. (g) Time = 3.0. (h) Time = 3.2. (i) Time = 3.4.

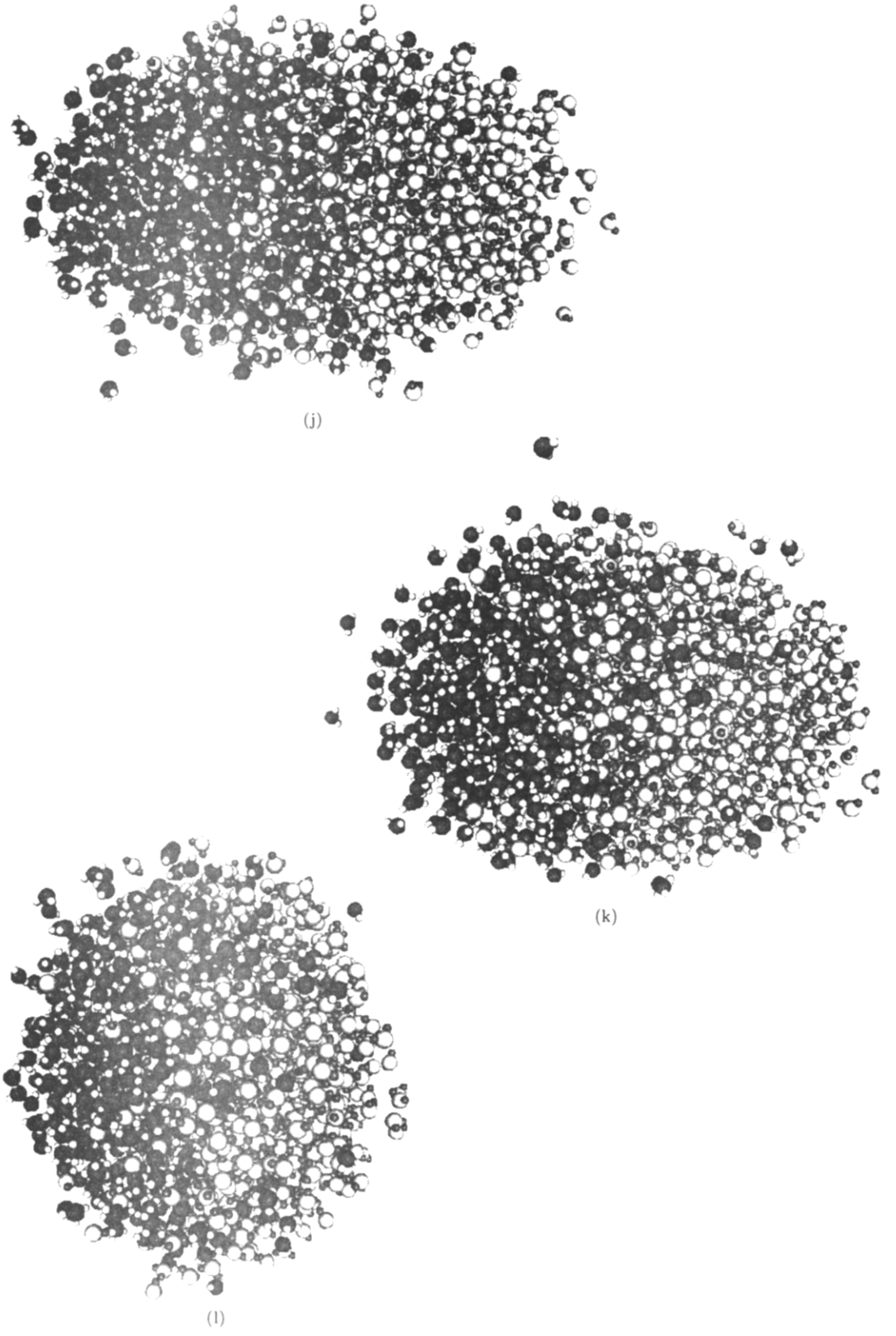

Figure 13. (j) Time = 3.8. (k) Time = 4.2. (l) Time = 4.6.

to rotate faster. This faster rotation caused the centripetal force on the outer molecules to become great enough to free them from the attractive forces of the central core.

Experiment 3 is shown in Figures 14–17. In these figures, a radius can be seen in which molecules inside this radius stay with the drop, and those outside are lost. As the molecules were being rapidly released, the system resembled a spiral galaxy. With increasing time, fewer molecules were released and the remaining drop became more and more spherical. This process was much slower than we had anticipated. Note that in Figure 17u, the time is at 55.5 picoseconds and the drop is still releasing molecules and is still not spherical. This suggested that a spiraling ellipsoid may be the dominant mode of oscillation for small drops since it is so slow to become spherical in comparison to the other modes of oscillation observed.

Note that to get the release of molecules during rotation, impact velocities must be within a certain range. If they are too slow, rotation will not be great enough to release molecules. If they are too fast, the drops will not coalesce. Related matters will be studied in Experiments 4 and 5.

Experiment 4

In this run, drops A and B were placed 3 Å apart. Drop A was given a velocity vector of (54,41,0) Å/ps and drop B was given a velocity vector of (−41,−54,0) Å/ps. This resulted in a high velocity, off-center collision that did not culminate in coalescence, but did produce satellites. As the drops collided, molecules were stripped off, leaving a trail of debris as the bulk of the drops continued on their way. The result was the formation of two smaller drops with smaller velocities and a trail of very small satellites. Experiment 4 is shown in Figures 18,19.

Experiment 5

In this run, drops A and B were placed 3 Å apart. Drop A was given a velocity vector of (6,34,0) Å/ps and drop B was given a velocity vector of (−6,−34,0) Å/ps. This resulted in a high velocity, brush type collision that does not yield coalescence. As the drops brush by one another, the surfaces of the drops are deformed and the directions of the drops' velocity vectors are turned in toward each other. But, as the drops separate, the surfaces again become spherical and no satellites are formed. In this experiment, through careful observation, one can see that the drops did not bounce apart, but slid past each other. Without this observation, in this type collision, the drops could be misconceived as bouncing apart. Experiment 5 is shown in Figures 20–22. It should also be noted that in Experiments 3,4, and 5 very little mixing occurred. Even the satellites produced in Experiment 4 tended to be made up of molecules from the same parent drop. With this in mind, to maximize mixing in a collision, the impact should be made as close to head-on as possible.

Experiment 6

In this run, drops A and B were placed 3 Å apart. Drop A had a velocity vector of (60,0,0) Å/ps and drop B had a velocity vector of (−60,0,0) Å/ps. This was a high speed, head-on collision. The result was the formation of a pancake shaped drop with the flat surface perpendicular to the original velocity vectors. From the edges of this pancake, a large number of molecules were released. The remaining molecules began to oscillate in the same fashion as in Experiments 1 and 2. Experiment 6 is shown in Figures 23–25. This experiment showed that drops of this size can coalesce under extreme conditions. Each drop in this experiment had a velocity of well over 13,000 miles per hour.

Experiment 7

We next wanted to compare the collision in Experiment 1 to a similar collision of a larger drop to determine if results would be similar. We learned when working with larger drops that

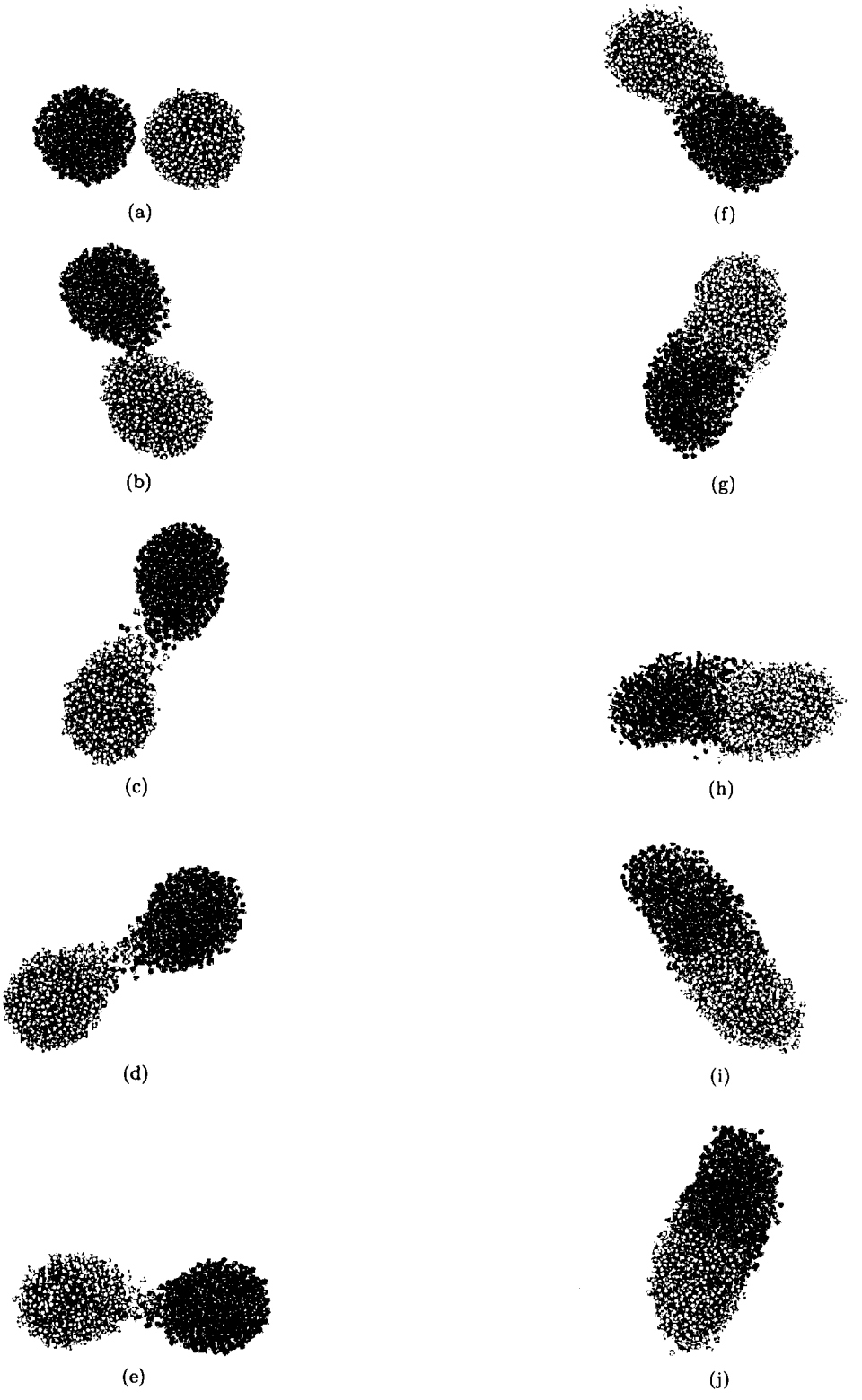

Figure 14. (a) Time = 0.0. (b) Time = 0.6. (c) Time = 1.2. (d) Time = 1.8. (e) Time = 2.4. (f) Time = 3.0. (g) Time = 3.6. (h) Time = 4.2. (i) Time = 4.8. (j) Time = 5.4.

Figure 15. (k) Time = 6.0. (l) Time = 6.6. (m) Time = 7.2. (n) Time = 7.8. (o) Time = 8.4. (p) Time = 9.0. (q) Time = 9.6.

(r)

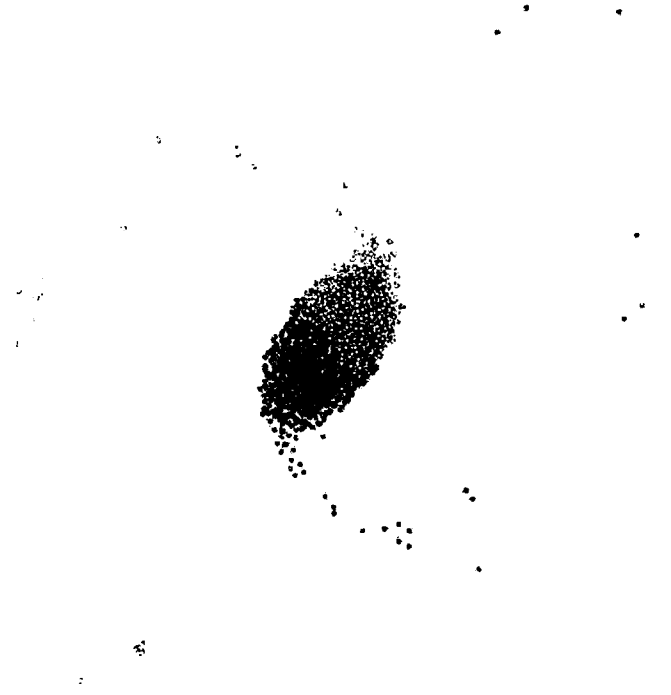

(s)

Figure 16. (r) Time = 10.2. (s) Time = 10.8.

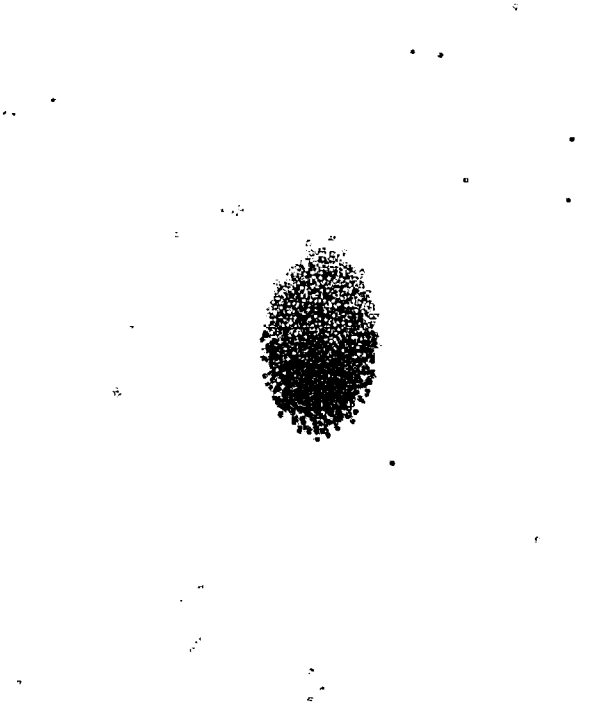

(t)

(u)

Figure 17. (t) Time = 13.8. (u) Time = 55.5.

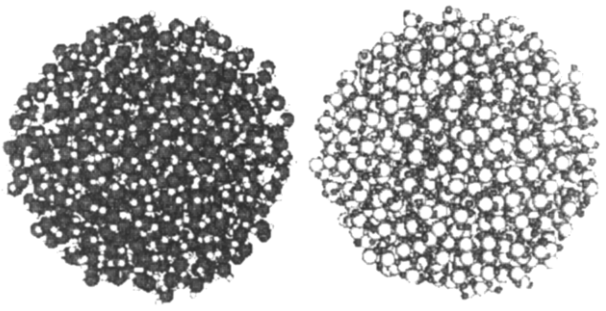

(a)

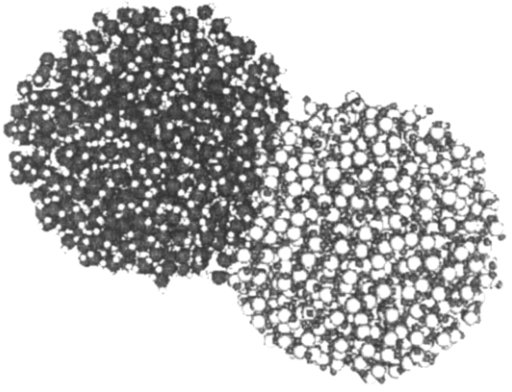

(b)

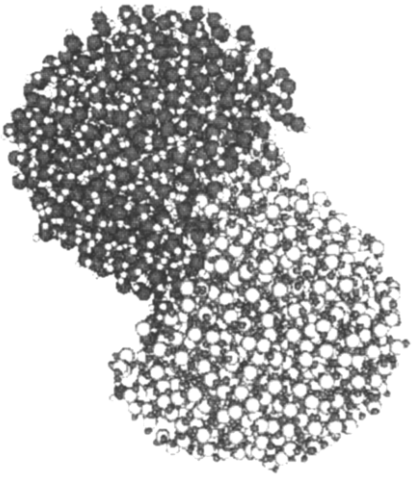

(c)

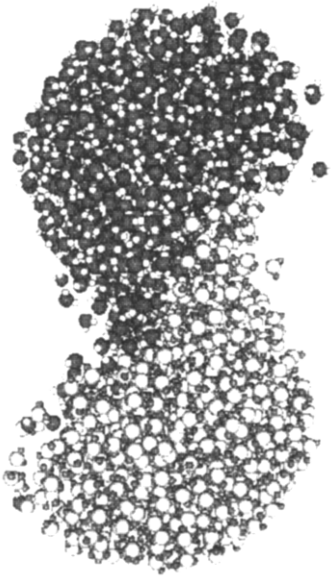

(d)

Figure 18. (a)Time = 0.0. (b) Time = 0.1. (c) Time = 0.2. (d) Time = 0.3.

(e)

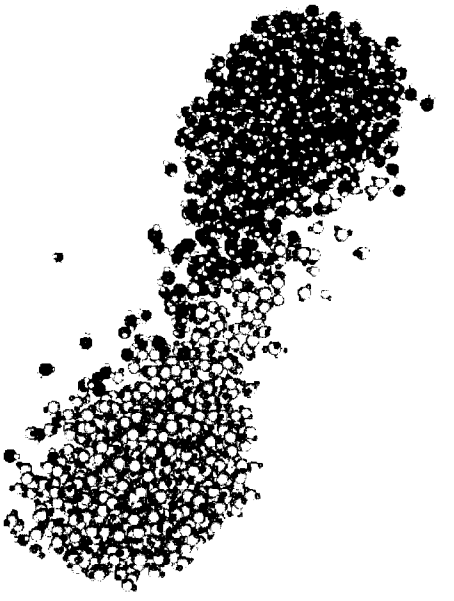

(f)

(g)

Figure 19. (e) Time = 0.4. (f) Time = 0.5. (g) Time = 0.9.

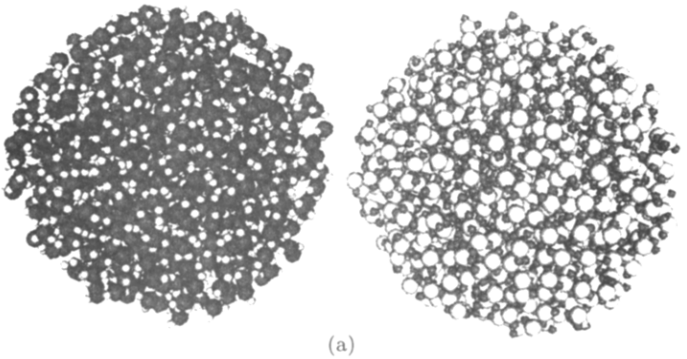

(a)

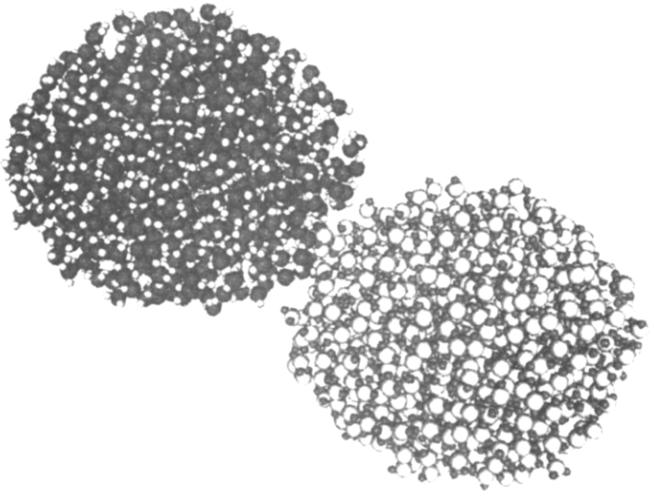

(b)

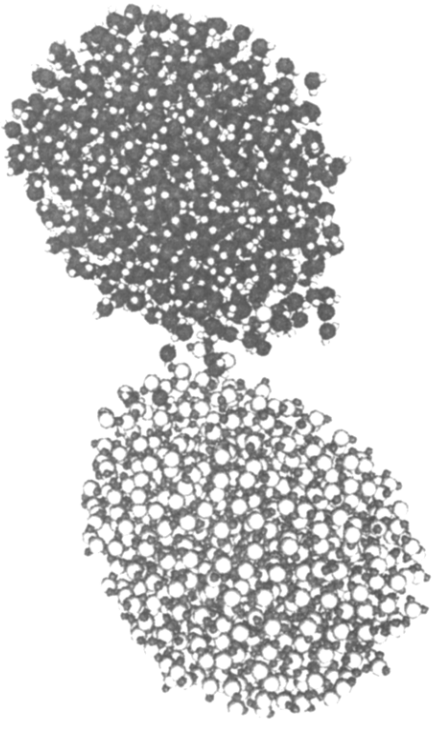

(c)

Figure 20. (a) Time = 0.0. (b) Time = 0.3. (c) Time = 0.6.

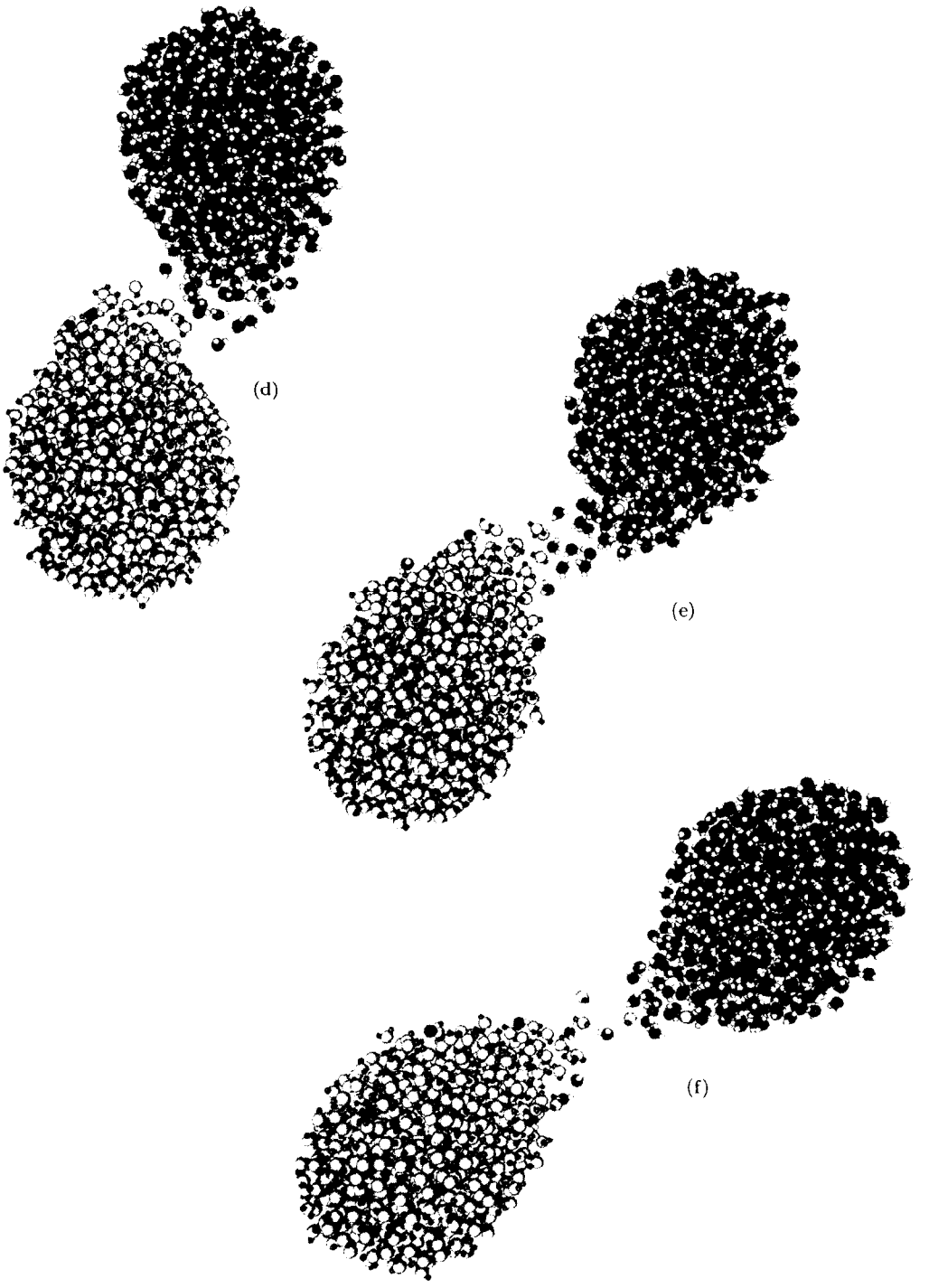

Figure 21. (d) Time = 0.9. (e) Time = 1.2. (f) Time = 1.5.

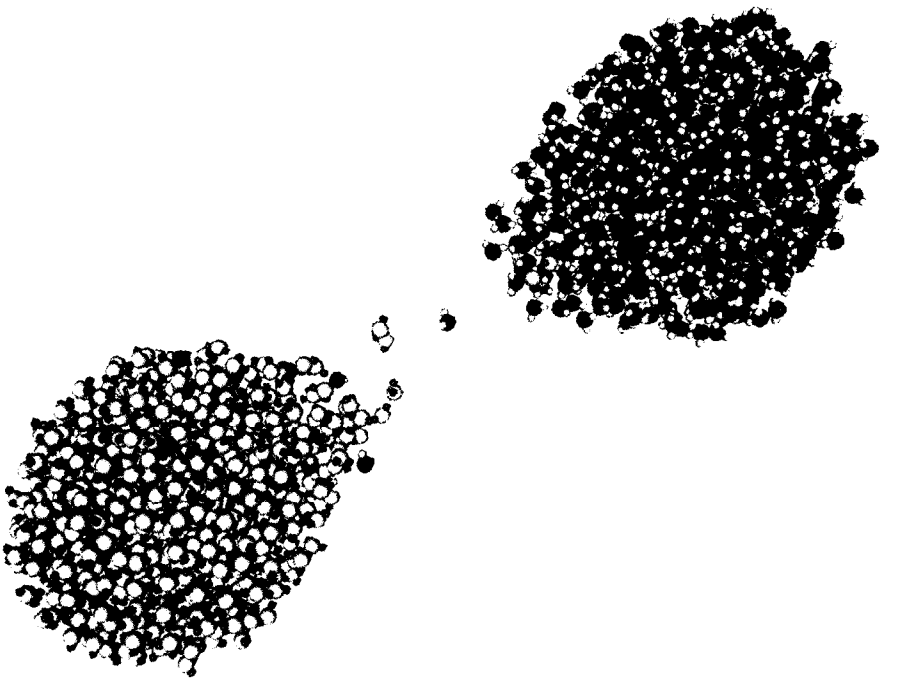

(g)

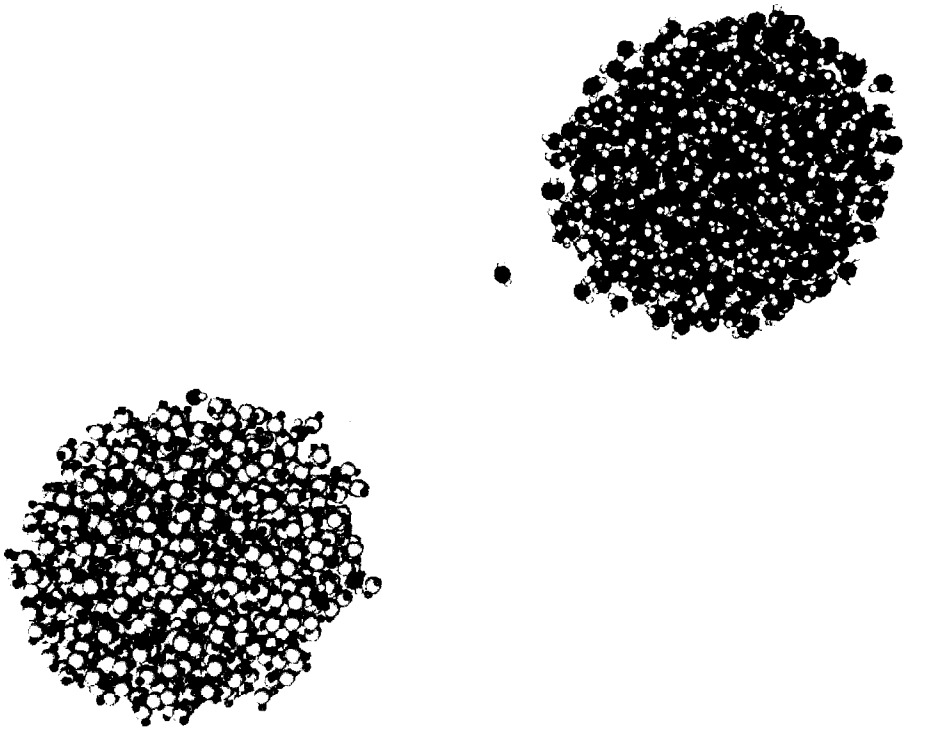

(h)

Figure 22. (g) Time = 1.8. (h) Time = 2.3.

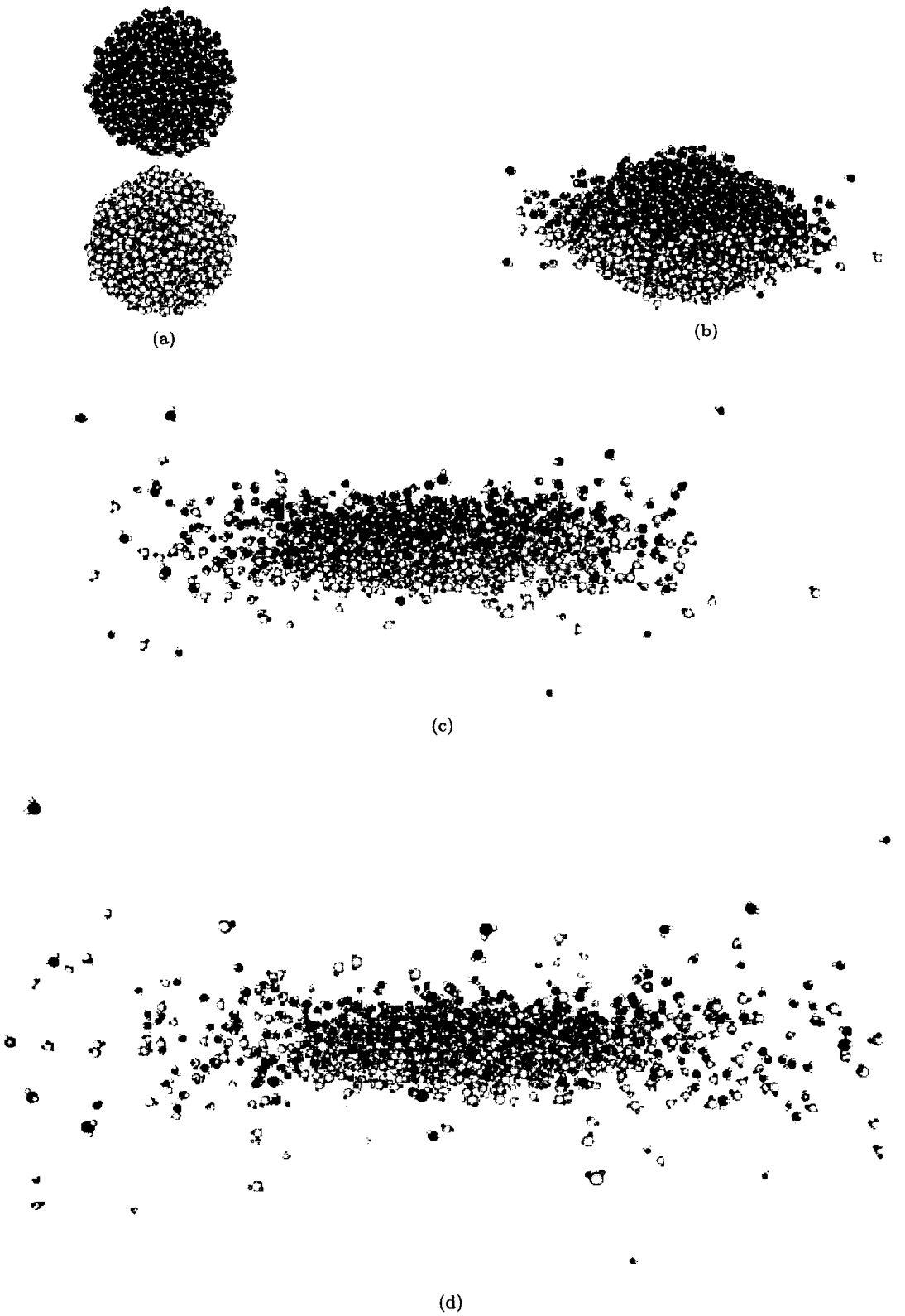

Figure 23. (a) Time = 0.0. (b) Time = 0.3. (c) Time = 0.6. (d) Time = 0.9.

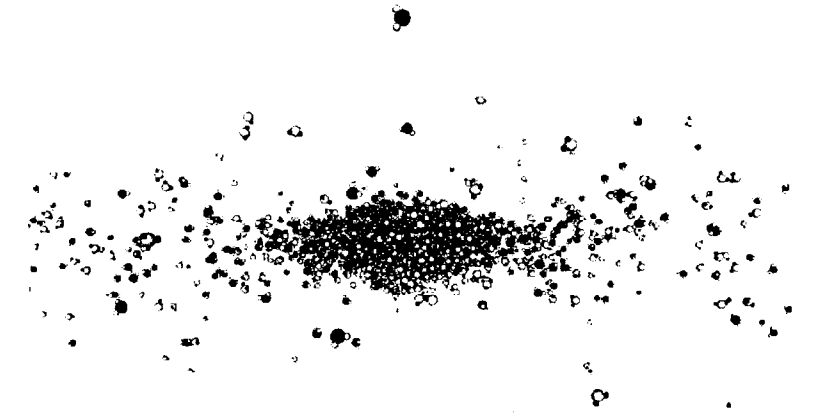

(e)

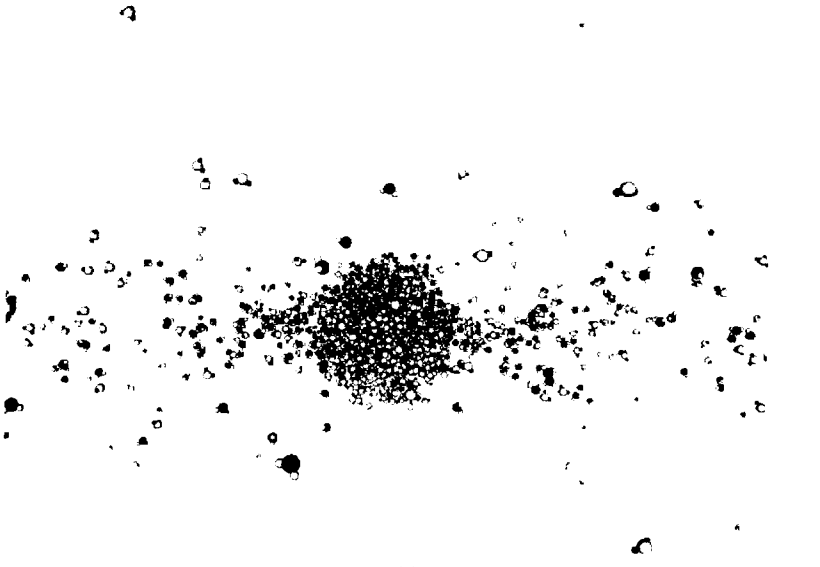

(f)

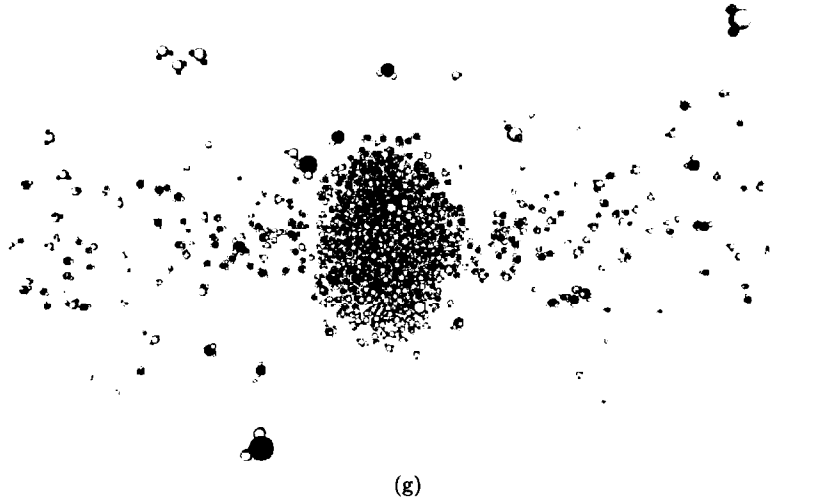

(g)

Figure 24. (e) Time = 1.5. (f) Time = 1.8. (g) Time = 2.1.

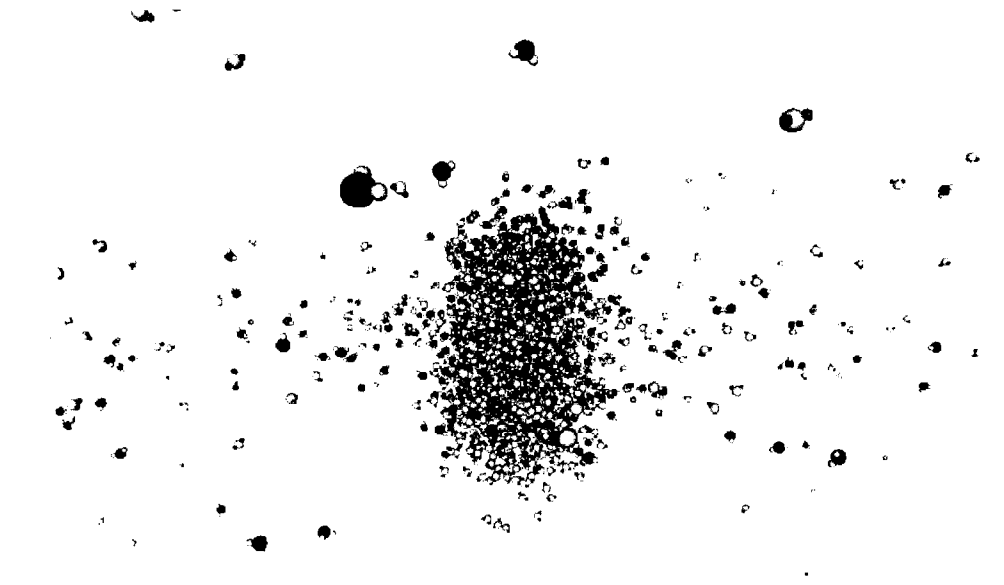

(h)

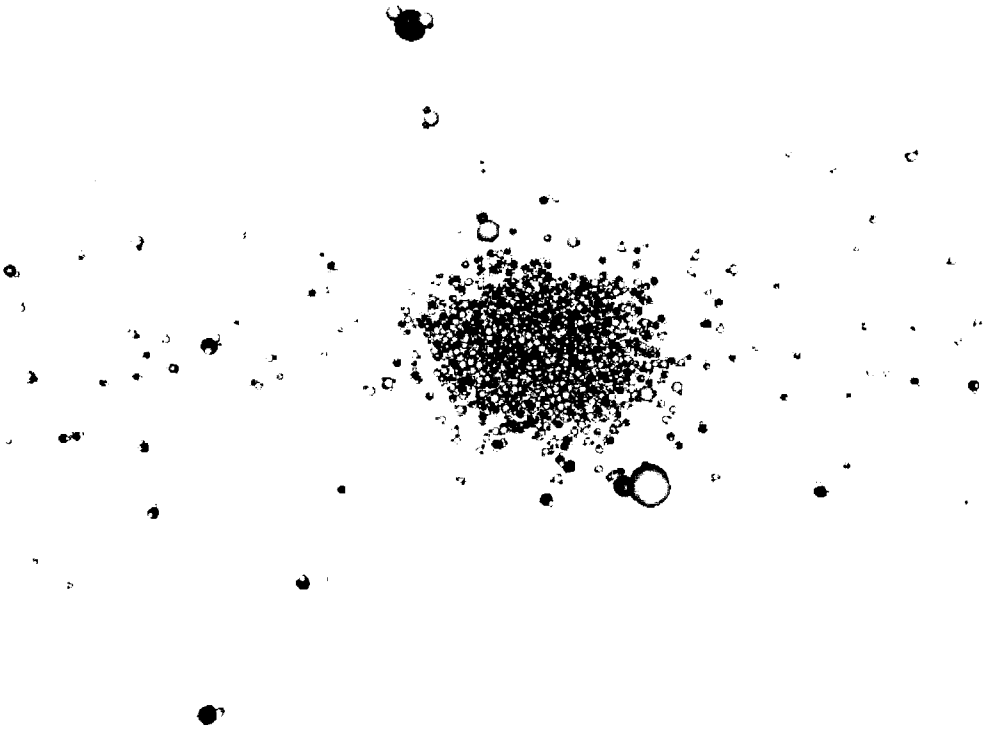

(i)

Figure 25. (h) Time = 2.7. (i) Time = 3.9.

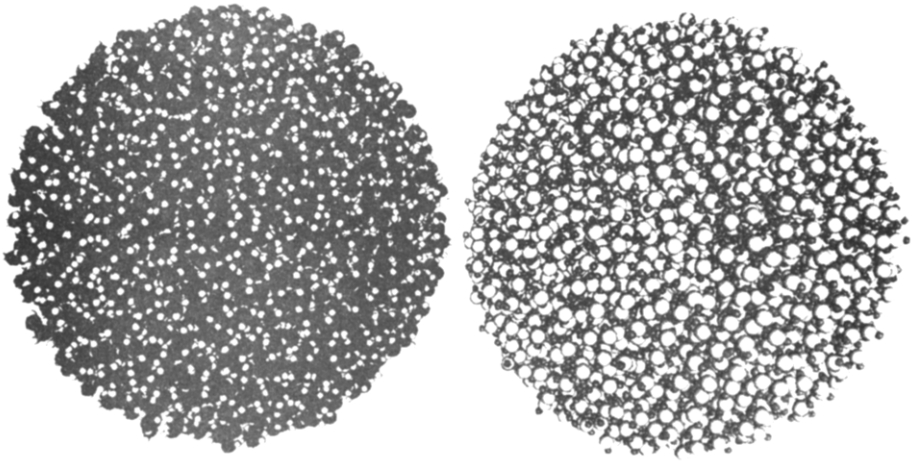

(a)

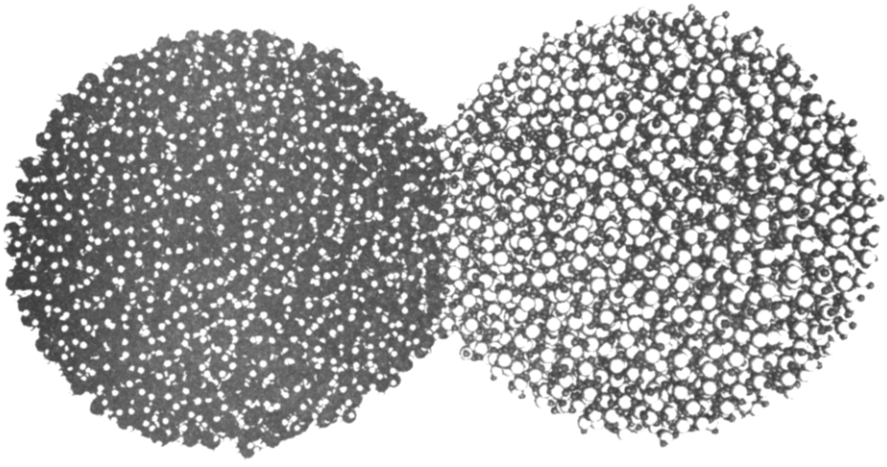

(b)

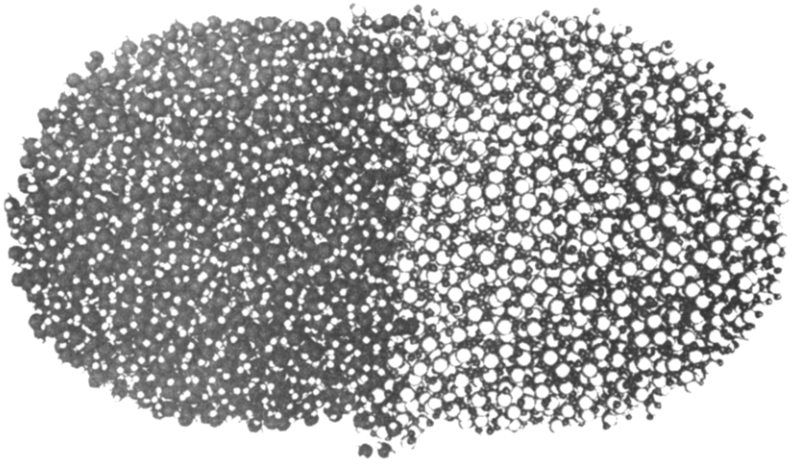

(c)

Figure 26. (a) Time = 0.0. (b) Time = 0.2. (c) Time = 0.4.

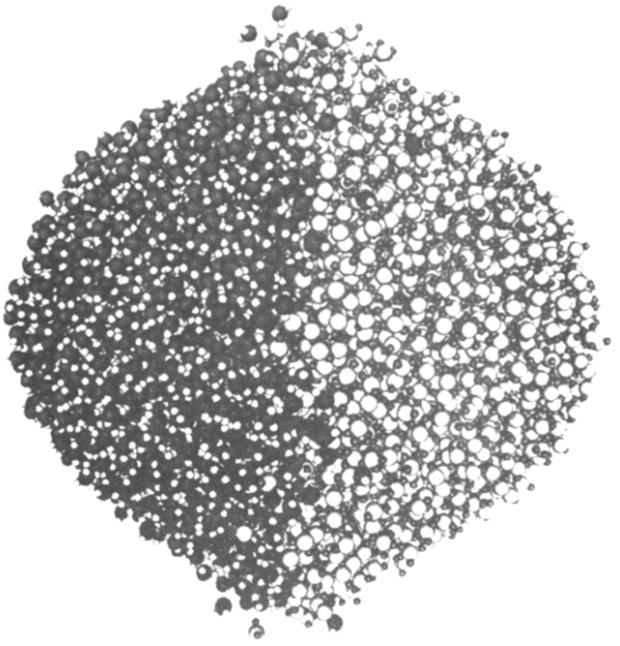

(d)

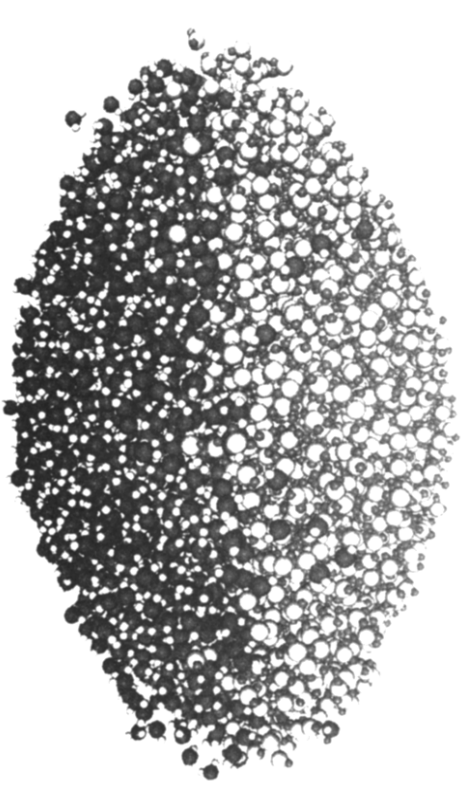

(e)

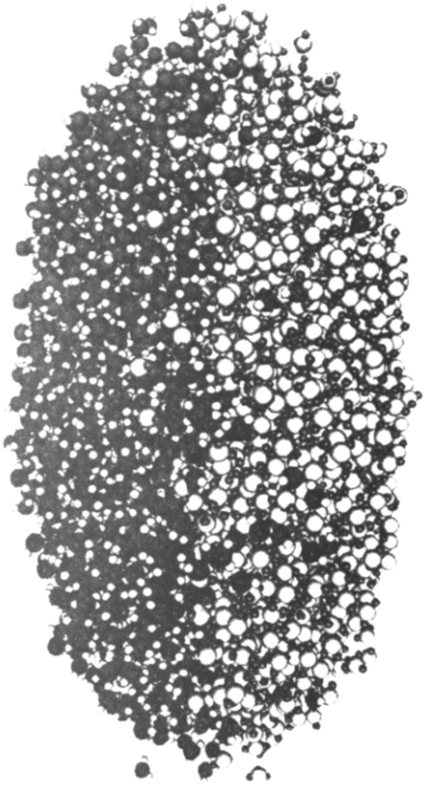

(f)

Figure 27. (d) Time = 0.6. (e) Time = 0.8. (f) Time = 1.0.

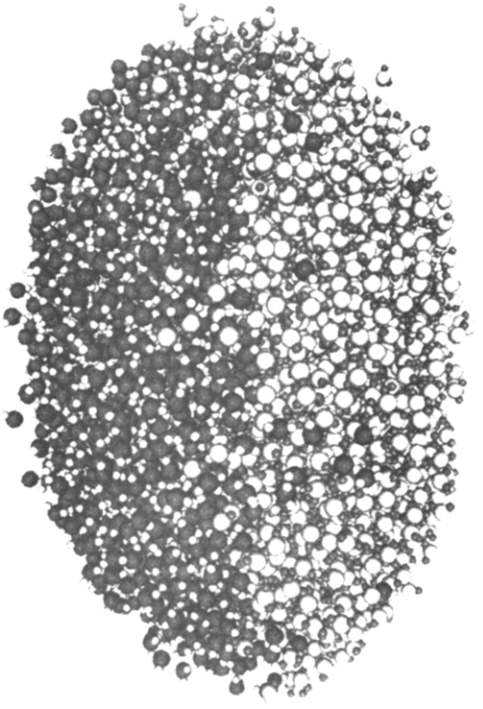

(g)

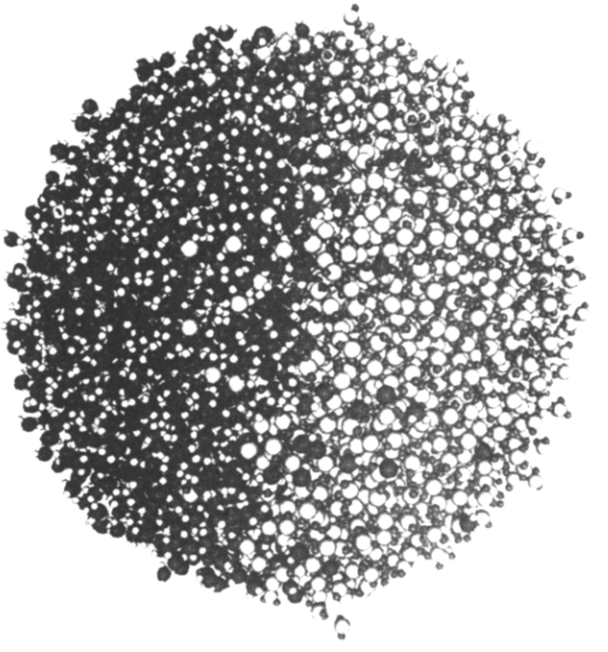

(h)

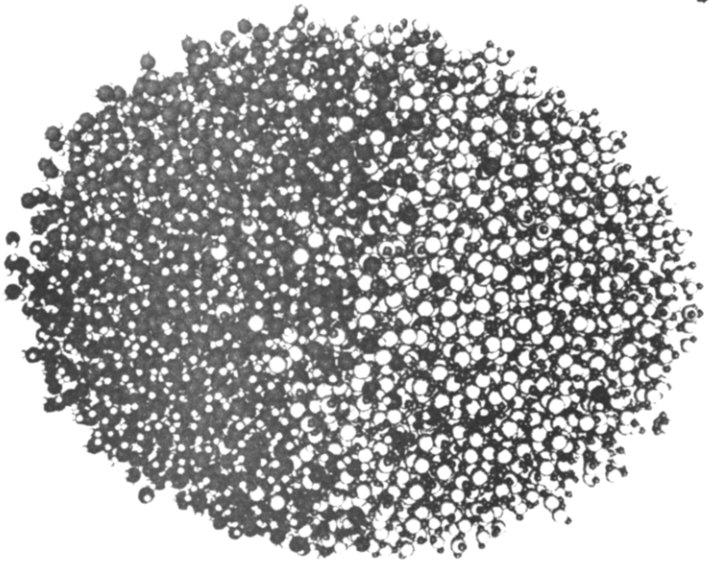

(i)

Figure 28. (g) Time = 1.2. (h) Time = 1.4. (i) Time = 1.6.

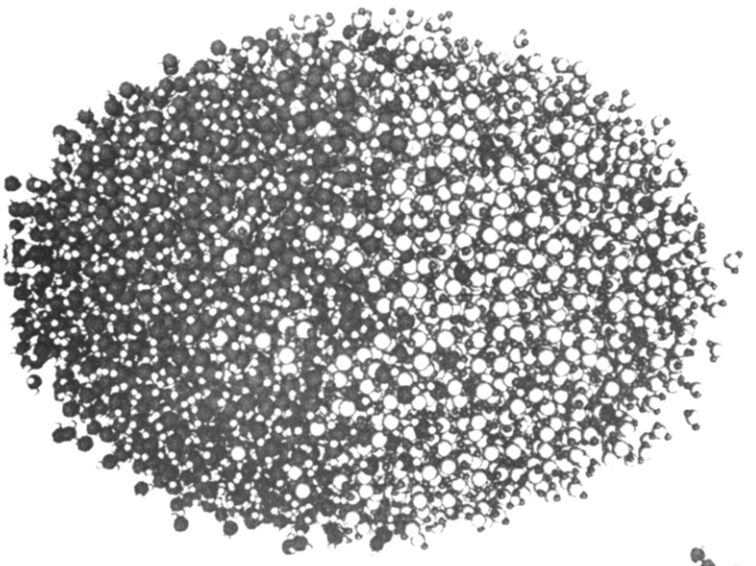

(j)

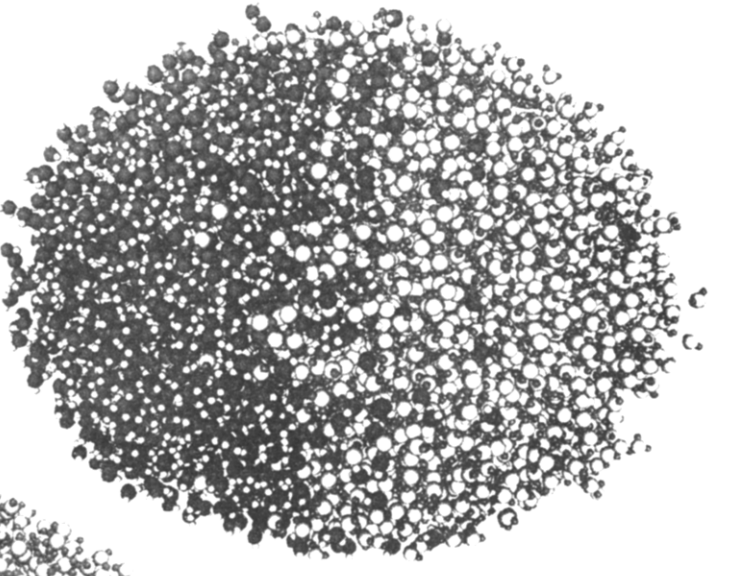

(k)

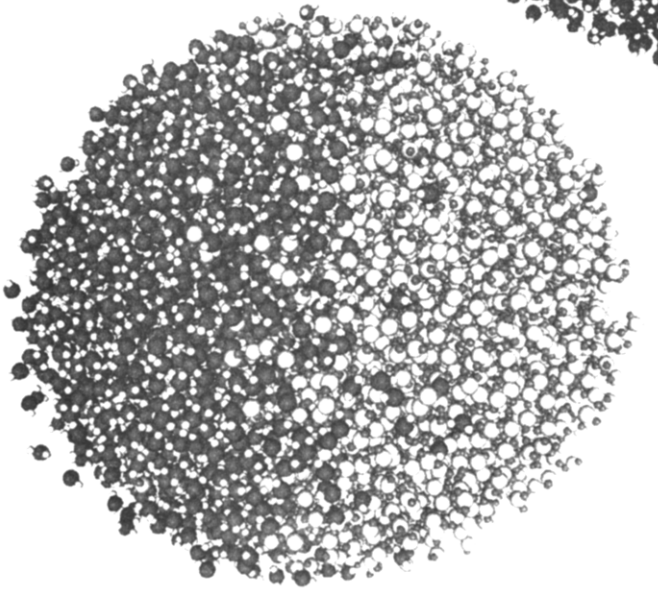

(l)

Figure 29. (j) Time = 1.8. (k) Time = 2.0. (l) Time = 2.2.

the probability of having a molecule dissociate greatly increases. This was cause for concern because, in the present HYB model, there is a singularity in the Coulombic attraction between oxygen and hydrogen atoms of different molecules. While the molecules are intact, this Coulombic divergence is prevented by the repulsive component of the Lennard-Jones forces between oxygen atoms. However, if a molecule dissociates, a free hydrogen atom could accelerate extremely fast toward a close oxygen atom and free its hydrogen atoms. This could start a chain reaction that would cause hydrogen atoms to be blown from the system and, on several occasions, this is exactly what happened. Hence, when working with larger drops, dissociation could not be ignored and the Coulombic singularity between the oxygen and hydrogen atoms of different molecules had to be addressed. To accomplish this, we added to our model the repulsive force component:

$$F(r) = \frac{23994.2}{r^{10}} \text{ uÅ/ps}^2$$

of the OH potential function of the CFM model [24]. Note that we rounded the exponent to 10 to increase computational speed. The addition of this force to our model slowed its overall computational speed very slightly because the addition of this force only removed the above singularity. We did not try to incorporate into our model accurate ionic components which we still felt played a negligible role in our experiments.

With this obstacle removed, we proceeded as follows: five of the A drops were place on the five vertices of two tetrahedrons which had a common base. The size of the tetrahedrons were chosen such that distance between each drop was approximately three angstroms. We then proceeded in the same manner as in Section 4 to produce two stable drops of 3645 molecules each.

These drops were placed three angstroms apart with zero drop velocities, and they oscillated in much the same fashion as the drops in Experiment 1. This collision is shown in Figures 26–29. Note that, to perform this experiment, a 21,870 body problem had to be solved numerically and, as a result, to simulate one picosecond took over 70 hours of CPU time on a CRAY Y-MP machine.

6. REMARKS AND CONCLUSIONS

This study showed how drop growth can be extremely rapid during cloud formation, but slows as the drops become larger; how collision and coalescence play a major role in drop formation; and the different shapes and modes of oscillation of drops. Another interesting fact observed was that these collisions of very small drops, simulated on a computer, closely resemble observed physical collisions of much larger drops of water. Hence, one can study the shapes and modes of oscillation of large drops by studying small drops on the computer. This is desirable because physical experiments are hard to set up and precise observations are difficult to obtain; but with computer experiments, all experimental parameters are simply computer inputs and precise observation, from almost any view point imaginable, can be made at any time through computer output.

This study has given great insight into what is occurring when small water drops are being formed. Computer simulations enable one to watch the actual atoms and molecules attract and repel one another, make and break hydrogen bonds, and to observe the molecules themselves form drop configurations. The computer can reveal details and insights into this small world that, at present, can be attained in no other way.

REFERENCES

1. I. Peterson, Raindrop oscillations, *Science News* **127**, 136 (1985).
2. C.D. Ahrens, *Meteorology Today*, West Publishing Company, St. Paul, (1985).
3. H.R. Byers, *General Meteorology*, McGraw-Hill Book Company, (1959).
4. H.G. Houghton, *Physical Meteorology*, Massachusetts Institute of Technology, (1985).

5. W.J. Humphreys, *Physics of the Air*, Dover Publications, (1964).
6. M. Neiburger, J.G. Edinger and W.D. Bonner, *Understanding Our Atmospheric Environment*, W.H. Freeman and Company, (1982).
7. A.L. Itkin, Macroscopic theory of evolution of liquid drops in natural vapor, *Journal of Mech. and Tech. Physics* **28**, 85 (1987).
8. H.L. Lemberg and F.H. Stillinger, Central-force model for liquid water, *Journal of Chemical Physics* **62**, 1677 (1975).
9. F.H. Stillinger, *Science* **209**, 451 (1980).
10. J.R. Adam, N.R. Lindblad and C.D. Hendricks, The collision, coalescence, and disruption of water droplets, *Journal of Applied Physics* **39**, 5173 (1968).
11. P.R. Brazier-Smith, S.G. Jennings and J. Latham, The interaction of falling water drops: Coalescence, *Proc. R. Soc. Lond. A.*, Vol. 326, p. 393, (1971).
12. S.F. Simpson and F.J. Holler, Effects of experimental variables on the mixing of solutions by collision of microdroplets, *Analytical Chemistry* **60**, 2483 (1988).
13. A. Miller, *Meterology*, Charles E. Merrill Books, Columbus, OH, (1966).
14. F.H. Stillinger and T.A. Weber, Amorphous state studies with the Gaussian core model, *Journal of Chemical Physics* **70**, 4879 (1979).
15. F.H. Stillinger and T.A. Weber, Lindemann melting criterion and the Gaussian core model, *Physical Review B* **22**, 3790 (1980).
16. D. Greenspan and L.F. Heath, Supercomputer simulation of the modes of colliding microdrops of water, *Journal of Physics D: Applied Physics* **24**, 2121 (1991).
17. F.H. Stillinger and A. Rahman, Improved simulation of liquid water by molecular dynamics, *Journal of Chemical Physics* **60**, 1545 (1974).
18. W.L. Jorgensen, J. Chandrasekhar, J.D. Madura, R.W. Impey and M.L. Klein, Comparison of simple potential functions for simulating liquid water, *Journal of Chemical Physics* **79**, 926 (1983).
19. W.L. Jorgensen and J.D. Madura, Temperature and size dependence for Monte Carlo simulations of TIP4P water, *Molecular Physics* **65**, 1381 (1985).
20. O.A. Karim and A.D.J. Haymet, *Journal of Chemical Physics* **89**, 6889 (1988).
21. H.J.C. Berendsen, J.P.M. Postma, W.F. van Gunsteren and J. Hermans, Interaction models for water in relation to protein hydration, In *Intermolecular Forces*, (Edited by B. Pullman), p. 331, Reidel, Dordrecht, Holland, (1982).
22. O.A. Karim, P.A. Kay and A.D.J. Haymet, The ice/water interface: A molecular dynamics simulation using the simple point charge model, *Journal of Chemical Physics* **92**, 4634 (1990).
23. A. Rahman, H.L. Lemberg and F.H. Stillinger, Study of a central force model for liquid water by molecular dynamics, *Journal of Chemical Physics* **62**, 5223 (1975).
24. F.H. Stillinger and A. Rahman, Revised central force potentials for water, *Journal of Chemical Physics* **68**, 666 (1978).
25. F.H. Stillinger and C.W. David, Polarization model for water and its ionic dissociation products, *Journal of Chemical Physics* **69**, 1473 (1978).
26. T.A. Weber and F.H. Stillinger, Solvating collisions between deuterons and light-water octamers, *Chemical Physics Letters* **89**, 154 (1982).
27. O.A. Karim, personal correspondence, November 9, 1990.
28. D.R. Lide, *CRC Handbook of Chemistry and Physics*, 72^{nd} edition, CRC Press, (1991).
29. D. Greenspan, *Quasimolecular Modelling*, World Scientific, (1991).
30. W.F. Van Gunsteren and H.J.C. Berendsen, Algorithms for macromolecular dynamics and constraint dynamics, *Molecular Physics* **34** (5), 1311 (1977).
31. J.O. Hirschfelder, C.F. Curtiss and R.B. Bird, *Molecular Theory of Gases and Liquids*, Wiley, New York, (1954).